PHYSICAL REVIEW B VOLUME 20, NUMBER 12 15 DECEMBER 1979

Bulk electronic structure of SiO_2

R. B. Laughlin* and J. D. Joannopoulos
Department of Physics, Massachusetts Institute of Technology, Cambridge, Massachusetts 02139

D. J. Chadi
Xerox Palo Alto Research Center, Palo Alto, California 94304
(Received 29 May 1979)

The electronic structures of crystalline and amorphous SiO_2 are examined via the tight-binding method. A new tight-binding Hamiltonian, fit to experiment and to the pseudopotential band structure of α quartz, is used to calculate densities of states for both α quartz and an SiO_2 Bethe lattice. These are shown to compare favorably with x-ray photoemission spectra of α quartz and amorphous SiO_2. The computational results are analyzed qualitatively using the bond-orbital approach. For both crystalline and amorphous SiO_2 it is suggested that oxygen $2s$ character in the lower conduction bands may be necessary to account for the large gap. Local symmetries of the lone-pair-like bands of possible relevance to the optical properties are discussed.

I. INTRODUCTION

This is the first in a series of papers concerned with the effects of inhomogeneities (disorder, defects, surfaces, and interfaces) on the electronic structure of SiO_2. Unlike the crystalline forms of SiO_2, which have been studied extensively[1–12] for many years, this important class of systems is relatively poorly understood on the microscopic level. There are two very different problems in these systems which set them apart from crystals: the absence of periodicity and the breakdown of the one-electron approximation. The first of these gives rise to the second, in the sense that disordered systems can possess both localized and extended states, and thus present correlation and mechanical relaxation effects potentially more difficult to understand than those of structural indeterminacy or randomness. Nevertheless, the two-problems are distinct physically and should be studied separately. In this and the following pages, the position will be adopted that understanding the first problem is a prerequisite for approaching the second.

Of the methods currently available for studying the effects of structural inhomogeneities on the density of states, one of the simplest is the cluster-Bethe-lattice technique.[13,14] Functionally the method entails simulating a random network calculation by embedding a small neighborhood from the network in Bethe lattices. Conceptually it is superior to the random-network approach in that it provides physical insight into the local origins of features in the density of states. The method has produced good agreement with experiment in studies of electrons in amorphous semiconductors[13] and in a recent theory of phonons in amorphous SiO_2.[15,16]

Realistic application of the cluster-Bethe-lattice method requires the existence of a tight-binding description of the bonding. Assuming that SiO_2 is fundamentally a bonded material and that methods appropriate for semiconductors are applicable to it, the first step in understanding disorder is to develop a tight-binding description of α quartz. The second step is to build an SiO_2 Bethe lattice and compare its density of states with photoemission for amorphous SiO_2.

In this paper, we deal with these two preliminary aspects of the inhomogeneity problem. In doing so, we develop a picture of SiO_2 which stresses the importance of the local atomic environment, and in which features of the electronic structure universal among all allotropes are identified. We go beyond previous local descriptions in that we explain the widths and shapes of the major bands as well as their centers of mass. This enables us to obtain a quantitative understanding of the formation of the fundamental gap in SiO_2, and suggests a new picture of bonding in SiO_2 in which oxygen $2s$ states play an important role. It also enables us to understand quantitatively the local symmetries of the states at the valence- and conduction-band edges, and thus shed light on the nature of the optical-absorption edge.

The plan of the paper is as follows. In Sec. II, we discuss the use of the Bethe lattice in studies of amorphous materials and outline its solution. In Sec. III, we discuss bonding in SiO_2, starting with the bond-orbital[2] picture. In Sec. IV, we compare the densities of states of α quartz and the Bethe lattice with experiment. In Sec. V, we discuss: (i) the relation between the shapes of the major bands, (ii) the symmetries of the states about the silicon centers, (iii) the disallowed nature of the first optical transi-

tions, and (iv) the role of the various tight-binding parameters in shaping the density of states. In Sec. VI, we discuss the ionicity of SiO_2 in the context of the formation of the fundamental gap, and the significance to the formation of the gap of the oxygen-2s wave-function admixture in the lowest conduction states. In Sec. VII, we discuss the effects of topological and bond-angle disorder in the glass. In Sec. VIII, we summarize our results.

II. BETHE LATTICE

A Bethe lattice is a bonded network of atoms which has the topology of a tree. The nearest-neighbor geometry and local environment of an atom are the same as those in the actual solid, but the ordinary necessity of having rings of bonds in the structure and fluctuations in the interaction parameters due to disorder is arbitrarily abolished. Although it is in many respects unphysical, the trivial topology of the Bethe lattice has been shown to be an excellent substitute for the disordered topology of a bonded glass.[17]

The SiO_2 Bethe lattice we deal with in this paper is depicted schematically in Fig. 1. Each silicon atom is tetrahedrally coordinated to four oxygen atoms, each oxygen atom is bonded to two silicon atoms, and the Si-O-Si angle is 144°. The Bethe lattice is identical to α quartz in every way except that it contains no closed rings of bonds.

We illustrate the solution of the Bethe lattice with an idealized form of SiO_2 in which each atom possesses only one s state. If the silicon and oxygen wave functions are denoted ψ_{Si} and ψ_O, then the simplified Hamiltonian is summarized as

$$\langle\psi_{Si}|H|\psi_{Si}\rangle = \epsilon_{Si} \ , \tag{1}$$

$$\langle\psi_O|H|\psi_O\rangle = \epsilon_O \ , \tag{2}$$

$$\langle\psi_{Si}|H|\psi_O\rangle = V \ , \tag{3}$$

$$\langle\psi_O|H|\psi_O'\rangle = V' \ , \tag{4}$$

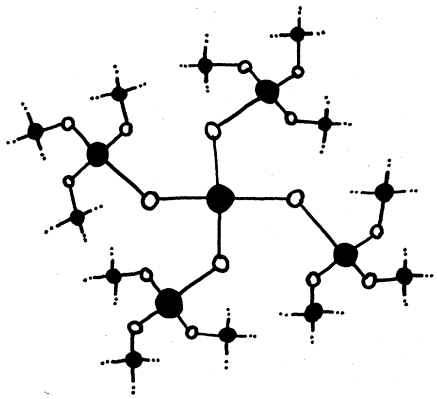

FIG. 1. Topology of the Bethe lattice. Every pair of atoms is connected by one and only one path of bonds.

We first renormalize away the silicon degree of freedom, effectively transforming the Hamiltonian into that of Weaire and Thorpe[18]

$$\langle\psi_O|\tilde{H}|\psi_O\rangle = \tilde{\epsilon}_O = \epsilon_O + \frac{2V^2}{\epsilon - \epsilon_{Si}} \ , \tag{5}$$

$$\langle\psi_O|\tilde{H}|\psi_O'\rangle = \tilde{V} = V' + \frac{V^2}{\epsilon - \epsilon_{Si}} \ . \tag{6}$$

This is depicted schematically in Fig. 2(a). We then confine the Hamiltonian to an O_4 molecule. As this has tetrahedral symmetry, the Hamiltonian is diagonalized trivially with one A_1 and three F_2 states

$$|A_1\rangle = \tfrac{1}{2}(|\psi_1\rangle + |\psi_2\rangle + |\psi_3\rangle + |\psi_4\rangle) \ , \tag{7}$$

$$|F_2\rangle = \tfrac{1}{2}(|\psi_1\rangle + |\psi_2\rangle - |\psi_3\rangle - |\psi_4\rangle) \ , \tag{8}$$

$$\vdots \qquad\qquad \vdots$$

the eigenvalues of which are

$$\epsilon_{A_1} = \tilde{\epsilon}_O + 3\tilde{V} \tag{9}$$

and

$$\epsilon_{F_2} = \tilde{\epsilon}_O - \tilde{V} \ . \tag{10}$$

The intramolecular Green's function is thus given by

$$G = \frac{1}{\epsilon - \epsilon_{A_1}}|A_1\rangle\langle A_1| + \frac{1}{\epsilon - \epsilon_{F_2}}\sum_j |F_2^j\rangle\langle F_2^j| \ . \tag{11}$$

Attaching the rest of the Bethe lattice is equivalent to adding an energy-dependent self-energy Z to each orbital. This gives

$$G = \frac{1}{\epsilon - \epsilon_{A_1} - Z}|A_1\rangle\langle A_1| + \frac{1}{\epsilon - \epsilon_{F_2} - Z}\sum_j |F_2^j\rangle\langle F_2^j| \ . \tag{12}$$

The diagonal Green's function matrix element associated with an oxygen orbital is thus

$$G_{11} = \frac{\frac{1}{4}}{\epsilon - \epsilon_{A_1} - Z} + \frac{\frac{3}{4}}{\epsilon - \epsilon_{F_2} - Z} \ . \tag{13}$$

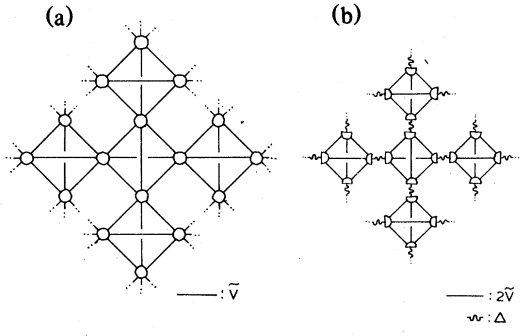

FIG. 2. Interaction diagram for the model Bethe lattice. (a) with silicon degree of freedom removed and (b) with each oxygen orbital replaced formally with two orbitals strongly bonded together.

Similar reasoning, however, may be applied to an isolated orbital. In the absence of the rest of the system, the Green's function of an orbital is

$$G_{11}=\frac{1}{\epsilon-\tilde{\epsilon}_0} \quad . \tag{14}$$

In the presence of the rest of the system, one has

$$G_{11}=\frac{1}{\epsilon-\tilde{\epsilon}_0-2Z} \quad . \tag{15}$$

The self-energy, Z, is thus determined by the condition

$$\frac{1}{\epsilon-\tilde{\epsilon}_0-2Z}=\frac{\frac{1}{4}}{\epsilon-\epsilon_{A_1}-2Z}+\frac{\frac{3}{4}}{\epsilon-\epsilon_{F_2}-Z} \quad . \tag{16}$$

The Bethe density of states is given by

$$\rho(E)=-\frac{1}{\pi}\,\mathrm{Im}\left(\frac{1}{\epsilon-\epsilon_0-2Z}\right) \quad . \tag{17}$$

The significance of the eigenvalues appearing in the denominators of Eq. (16) may be easily understood in terms of the unbonded Weaire-Thorpe system, shown in Fig. 2(b). This Bethe lattice, which is a system of interacting O_4 molecules, is equivalent to the one on the left in the limit of large Δ. Up to a self-energy shift of $-\Delta$, the A_1 and F_2 eigenvalues of a molecule are

$$\epsilon'_{A_1}=2\epsilon_{A_1}-\tilde{\epsilon}_0 \quad , \tag{18}$$

$$\epsilon'_{F_2}=2\epsilon_{F_2}-\tilde{\epsilon}_0 \quad . \tag{19}$$

Substituting

$$Z=\tfrac{1}{2}(\epsilon-\epsilon_0)+\tfrac{1}{2}\delta \tag{20}$$

into Eq. (16) we obtain

$$-\frac{1}{2\delta}=\frac{\frac{1}{4}}{\epsilon-\epsilon'_{A_1}-\delta}+\frac{\frac{3}{4}}{\epsilon-\epsilon'_{F_2}-\delta} \quad . \tag{21}$$

Thus, the parameters of the system influence its density of states *only* through the eigenvalues of the isolated O_4 molecule. These may be shown by explicit solution of Eq. (21) to delimit the band edges.

When a more realistic Hamiltonian is substituted for the simplified one, the analysis in the foregoing section remains basically unchanged but for the substitution of matrices for scalars. An alternative method of solution has been discussed recently.[16]

III. BONDING IN SiO_2

It has been shown by Pantelides and Harrison[2] that the electronic structure of SiO_2 can be understood simply in terms of the electronic levels of a small bonding unit containing an oxygen atom and one sp^3 hybrid from each adjacent silicon atom. Their picture is illustrated in the upper half of Fig. 3. The three $2p$ orbitals on the oxygen interact with the hybrids to form five *bond orbitals.* The oxygen-p state perpendicular to the bonding plane becomes the lone-pair bond orbital at the O-$2p$ level. The remaining nonbonding oxygen p interacts with the symmetric combination of hybrids to form the weak-bonding and weak-antibonding bond orbitals. As this interaction reduces to zero when the Si-O-Si angle is increased to 180°, the amount of mixing is fairly small. The oxygen p pointing along the bond interacts with the antisymmetric combination of hybrids to form the strong-bonding and strong-antibonding bond orbitals. The six electrons available for bonding then fill the system up to the lone pairs, which thus form the upper valence bands. The gap lies between the lone-pair and weak-antibonding energies, which is approximately the difference between the oxygen-$2p$ and silicon hybrid levels.

If the interaction between adjacent hybrids on the same silicon, as well as those between nearest-neighbor oxygen atoms, are sufficiently weak, bond orbitals will interact effectively only with others of the same species. This is illustrated in the lower half of Fig. 3. To an excellent approximation, bond orbitals interact only when they are adjacent, and always with the same interaction $\tilde{V}$. Thus the Hamiltonian which describes the broadening of a bond orbital into a band is always the same, up to the magnitude of $\tilde{V}$, which determines the bandwidth. By inspection, as-

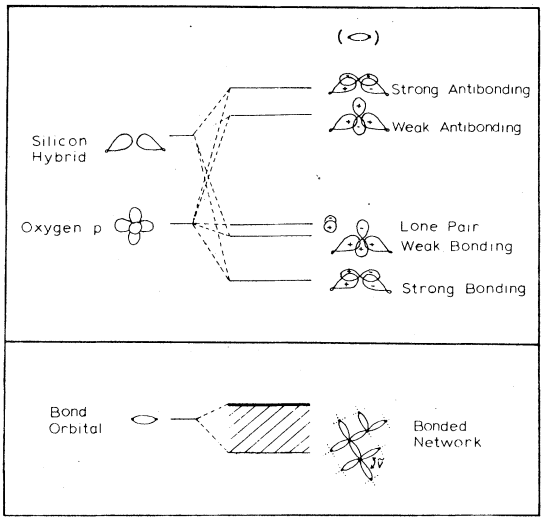

FIG. 3. Bond-orbital picture of band formation in SiO_2. Silicon hybrids and oxygen-$2p$ states interact (top) to form five bond orbitals, each of which subsequently broadens (bottom) into a band of characteristic shape. The width of this band scales with the nearest-neighbor interaction, $\tilde{V}$.

suming no odd-fold rings of bonds, the completely bonding state is lowered by $6\tilde{V}$, while the antibonding state is raised by $-2\tilde{V}$. This delimits the band. As the center of mass is unshifted, the antibonding states must be always more dense than the bonding states.

In Sec. VI, we shall criticize the bond-orbital picture just described on the grounds that it excludes oxygen-2s states. We remark at this point that their inclusion does not alter the picture qualitatively. Even if bonding between these states and silicon hybrids is important, symmetry allows only the weak-bonding and weak-antibonding bond orbitals to be affected. Since the weak-bonding state contains almost no silicon character, however, the primary effect of including oxygen-2s—silicon hybrid interactions is to push the oxygen-s and weak-antibonding levels apart while mixing their characters slightly. This has also been noted by Yndurain.[19]

IV. DENSITIES OF STATES

Experimentally,[1,12,20–23] the electronic structures of crystalline and amorphous SiO_2 are known to be very similar. In Fig. 4, we compare x-ray photoemission spectra[20] of the crystal and the glass. In each case, one sees two distinct bands, one composed of both weak-bonding and lone-pair states (0–5 eV) and another which is strong bonding (6–11 eV) in character. The widths of these bands are the same in both materials, as are their overall shapes. There is structure in the strong-bonding band of α quartz near 9 eV which is absent in amorphous silica, but the peak at 6 eV is present in both spectra. The lone-pair-like band tends to lose some fine structure and peak up slightly in the center as the material is made amorphous.

In Fig. 5, we show theoretical densities of states for α quartz and the Bethe lattice calculated using the empirical tight-binding Hamiltonian listed in Table I. In each case one sees four distinct bands: the oxygen-s states (−22 to −19 eV), the strong-bonding states (−11 to −6 eV), the lone-pair-like band (−5 to 0 eV), and the weak-antibonding conduction states (10 eV and above). There is structure in the center of the strong-bonding band of α quartz near −9 eV which is absent in the Bethe lattice, but the spike near −6 eV is present in both densities of states. This effect is also seen in the oxygen s and lower conduction bands. There is virtually no change in the long-pair-like band when the Bethe lattice is substituted for α quartz.

The calculated band structure of α quartz along the principal symmetry directions of the Brillouin zone is shown in Fig. 6. As the pseudopotential[3] calculation gives the wrong splitting between the oxygen-s and strong-bonding bands, this distance has been fit to

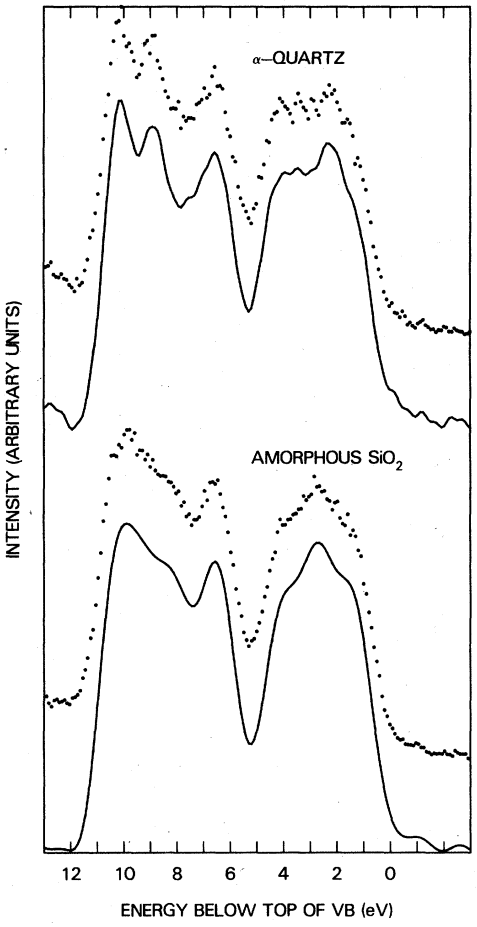

FIG. 4. X-ray photoemission spectra of α quartz (top) and amorphous silica (bottom) taken from Ref. 18. The solid curves are smoothed versions of the data, shown in dots.

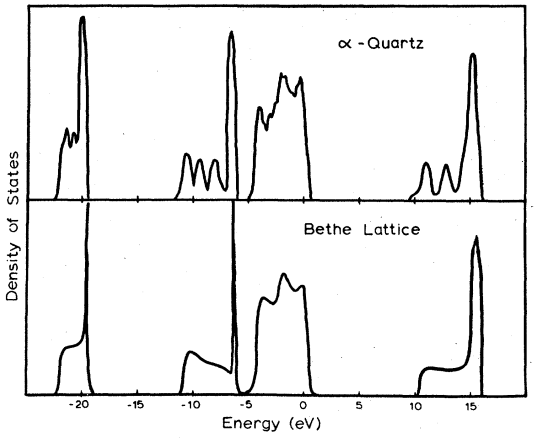

FIG. 5. Densities-of-states α quartz and the Bethe lattice calculated using the Hamiltonian listed in Table I.

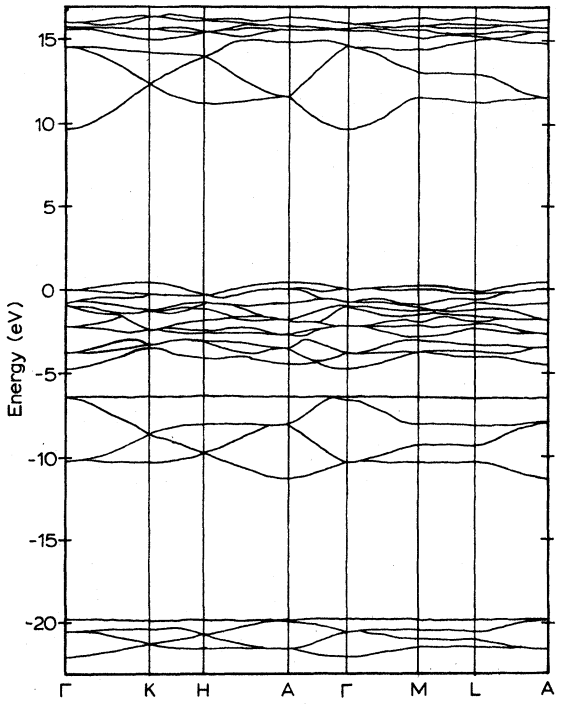

FIG. 6. Band structure of α quartz calculated using the Hamiltonian listed in Table I.

x-ray emission[23] and x-ray-photoemission (XPS)[20] data. The gap is indirect (A to Γ) and has a magnitude of 9.2 eV. The ordering of the degeneracies at symmetry points agrees with the pseudopotential except in the lone-pair-like bands. The bands are sufficiently dense in this region that simultaneously fitting the density of states and the ordering of the degeneracies is impossible with the parameterization we have chose. The dispersion of the remaining bands shows considerable duplication. The oxygen-s, strong-bonding, and lower conduction regions all contain six bands, only 3 of which disperse significantly. These 3 clearly scale between the oxygen-s and lower conduction bands but have their degeneracies reversed in the strong-bonding bands. This reversal is due to the negative phase between the silicon hybrids in the bond orbital. In each of these three regions, the remaining nondispersive bands induce a large density of states at the upper edge of the band.

The parameters used in the tight-binding Hamiltonian are summarized in Table I. The basis set consists of Si-3s, Si-3p, O-2s, and O-2p states only. All possible nearest-neighbor, Si-O interactions are included, as are small nearest-neighbor O-O interactions. The criteria for determining the parameters in Table I are discussed in Sec. V.

TABLE I. Tight-binding parameters for SiO_2. Oxygen-oxygen parameters are defined relative to the O-Si-O bonding plane. Oxygen-p orbitals in the plane may lie either along the bond or perpendicular to it. The possible in-plane interactions allowed by symmetry are parameterized by V_1^0 through V_3^0.

$\langle \text{Si } s \vert H \vert \text{Si } s\rangle = 4.95$	$\langle \text{O } s \vert H \vert \text{O } s\rangle = -16.4$
$\langle \text{Si } p \vert H \vert \text{Si } p\rangle = 11.2$	$\langle \text{O } p \vert H \vert \text{O } p\rangle = -1.3$
$\langle \text{Si } s \vert H \vert \text{O } s\rangle = -3.05$	$\langle \text{O}' \vert H \vert \text{O}\rangle$: $V_1^0 = 0.574$
$\langle \text{Si } p \vert H \vert \text{O } s\rangle = -7.0$	$V_2^0 = -0.548$
$\langle \text{Si } s \vert H \vert \text{O } p\rangle = -5.4$	$V_3^0 = -0.75$
$\langle \text{Si } p \vert H \vert \text{O } p\rangle_\sigma = 5.4$	$V_4^0 = 0.26$
$\langle \text{Si } p \vert H \vert \text{O } p\rangle_\pi = -1.4$	$V_5^0 = -0.45$

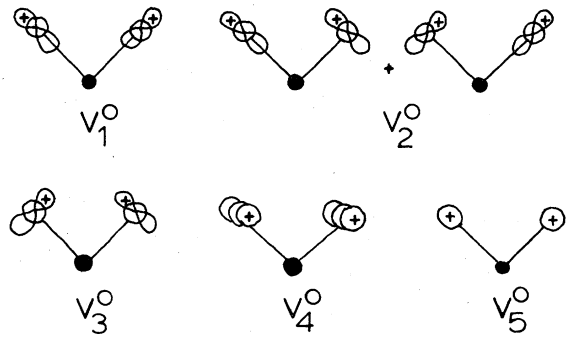

V. BAND SHAPES

The oxygen-s, strong-bonding, and lower conduction bands have in common a characteristic shape in the Bethe lattice which carries over to α quartz, up to additional superimposed structure. These bands all derive from a single bond orbital and are thus described by the bonding part of the Weaire-Thorpe Hamiltonian.[18] The solution of the Bethe lattice using this Hamiltonian has been outlined in Eqs. (5)–(21). If $\tilde{\epsilon}_O$ is the energy of the bond orbital and $\tilde{V}$ is the interaction between two bond orbitals in the same tetrahedron, then one may substitute

$$\epsilon'_{A_1} = \tilde{\epsilon}_O + 6\tilde{V} \ , \tag{22}$$

$$\epsilon'_{F_2} = \tilde{\epsilon}_O - 2\tilde{V} \ , \tag{23}$$

into Eq. (21) to obtain the density of states. The symmetry of the states about the silicon centers is reflected in the local densities of states, the density of states weighted by the square of the amplitude of

each state on an A_1 or F_2 combination of bond orbitals. These are given by

$$\rho_{A_1}(\epsilon) = -\frac{2}{\pi}\,\mathrm{Im}\left[\frac{1}{\epsilon - \epsilon'_{A_1} - \delta}\right] , \tag{24}$$

$$\rho_{F_2}(\epsilon) = -\frac{2}{\pi}\,\mathrm{Im}\left[\frac{1}{\epsilon - \epsilon'_{F_2} - \delta}\right] . \tag{25}$$

We have

$$\rho(\epsilon) = \tfrac{1}{4}\rho_{A_1}(\epsilon) + \tfrac{3}{4}\rho_{F_2}(\epsilon) . \tag{26}$$

In Fig. 7, we show the solutions to these equations for $\epsilon_O = 0$ and $V = -1$. The characteristic asymmetry seen in these three bands is accurately reproduced. The states at the bonding edge may be seen to have pure A_1 character, while the antibonding states are pure F_2. X-ray emission spectroscopy,[23] which probes the local densities of states, verifies this $A_1 - F_2$ asymmetry for both the oxygen-s and strong-bonding bands: The lower edges of both are enhanced in the Si $L_{2,3}$ spectrum, while the upper edges are enhanced in the Si $K\beta$.

It is clear from Fig. 5 that the three-peak structure of the lone-pair-like band also results from local symmetries which are preserved in the Bethe lattice. Its shape can be understood in the following manner. As the width of the lone-pair-like band, which is due almost entirely to the oxygen-oxygen interactions, is much greater than the splitting between the lone-pair and weak-bonding bond orbitals, it is appropriate to treat this splitting as a perturbation to the system in which the Si-O-Si angle is 180°. This approximate system may be further idealized by formally removing all unnecessary orbitals: all those except the oxygen p states perpendicular to the bond. The model thus formed may be solved exactly by analogy with Eqs. (5)–(21). Each oxygen orbital is split in half, and each half assigned to each adjacent O_4 molecule. The transformed Hamiltonian, confined to a molecule, then splits the molecule into energy eigenstates, the eigenvalues of which appear in the denominators of Eq. (21). In this case, however, there are eight degrees of freedom in the molecule and three energy eigenvalues: a doubly-degenerate E state, a triply-degenerate F_2 state, and a triply-degenerate F_1 state. The analog of Eq. (21) for the lone-pair-like band is thus

$$-(2\delta)^{-1} = \tfrac{2}{8}(\epsilon - \epsilon'_E - \delta)^{-1} + \tfrac{3}{8}(\epsilon - \epsilon'_{F_2} - \delta)^{-1} + \tfrac{3}{8}(\epsilon - \epsilon'_{F_1} - \delta)^{-1} . \tag{27}$$

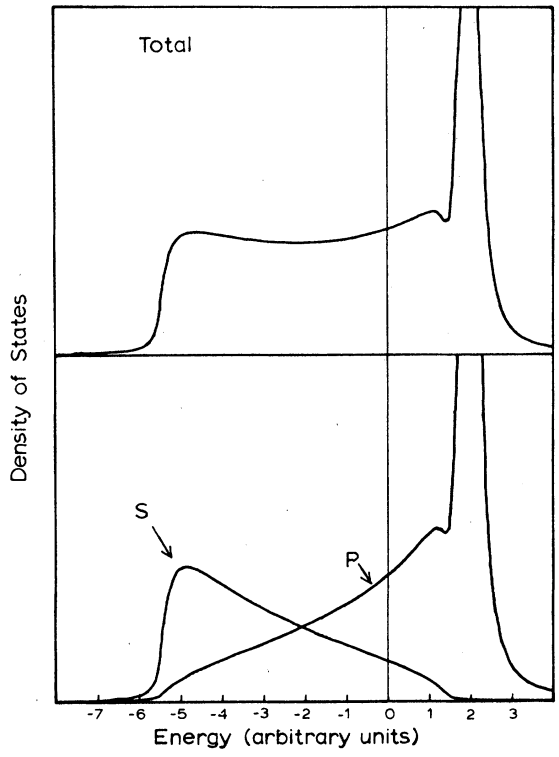

FIG. 7. Solutions of Eqs. (24)–(26), representing the density of states and orbital symmetries of an idealized bond-orbital-derived band.

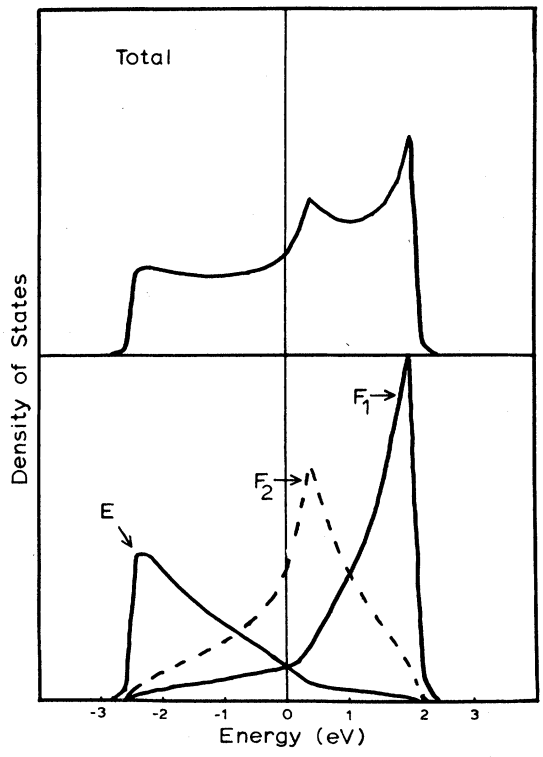

FIG. 8. Solution of Eq. (27), representing the density of states and orbital symmetries of an idealized lone-pair-like band.

In Fig. 8, we show the solution to Eq. (27) together with the E, F_1, and F_2 local densities of states. The eigenvalues are those resulting from the oxygen-oxygen interactions listed in Table I, with the O_{2p} energy set to zero. The shape is very similar to that seen in Fig. 5. There are two disparities, excessive strength near 2 eV and the lack of a discernable peak at -2 eV, both of which result from the absence of the Si-O-Si bend.

The oxygen-oxygen interactions have been fit to order the eigenvalues in the manner

$$\epsilon_E < \epsilon_{F_2} < \epsilon_{F_1} \tag{28}$$

as this is the ordering found in two less empirical calculations performed for the SiO_4 molecule.[4,9] We emphasize, however, that this ordering is also consistent with the pseudopotential results.[3] The pseudopotential density of states in this region is asymmetric, the low-energy side being smaller. This would indicate that the eigenvalue with the smallest degeneracy is the most deeply bound. In addition, the first direct optical transitions in the pseudopotential calculation appear to be dipole forbidden, even though no crystal structure selection rule is responsible. As the lowest conduction states have s-like, symmetry about the silicon centers, the location of the F_1 states, which is d-like, at the valence-band maximum would account very nicely for this selection rule. Based on this interpretation, we would predict that *the first direct transitions are forbidden in any allotrope of SiO_2 in which the SiO_4 tetrahedra remain intact.*

The model calculations discussed in this section demonstrate that parameterizing the density of states of SiO_2 effectively reduces to parameterizing a set of 11 eigenvalues, which lie at the major band edges and at peaks in the density of states. These include the A_1 and F_1 eigenvalues of the oxygen-s, strong-bonding, weak-antibonding, and strong-antibonding bands as well as the E, F_1, and F_2 eigenvalues of the lone-pair-like band. They may be obtained as eigenvalues of five small matrices having tight-binding parameters as elements. These are listed in Table II. Although the table is strictly valid only when the Si-O-Si angle is 180°, it is generally helpful in showing the approximate functions of the various parameters. For example, the π interaction, which is not included in the bond-orbital picture at all, may be seen from Table II to couple silicon p states to the F_2 combination of lone-pair-like orbitals. It primarily causes the latter to interact virtually with itself and with the p-like spike of the strong-bonding band. This results in an apparent shift of its energy and a shifting and severe broadening of the spike. Table II also shows that the oxygen-oxygen parameters V_2^0 has a similar effect. The fact that this spike is fairly sharp in the pseudopotential results indicates that either these parameters are small or their effects cancel.

All of the necessary eigenvalues but two may be obtained from the pseudopotential density of states or from experiment. The remaining two fall somewhere in the upper conduction bands beyond 15 eV, where both the pseudopotential and tight-binding calculations are unreliable. For want of a better value,

TABLE II. Six small matrices, the eigenvalues of which determine peaks and band edges in the Bethe-lattice density of states.

$$2A_1: \begin{pmatrix} \langle \mathrm{O}\ s|H|\mathrm{O}\ s\rangle + 6V_5^0 & \sqrt{8}\langle \mathrm{O}\ s|H|\mathrm{Si}\ s\rangle \\ \sqrt{8}\langle \mathrm{Si}\ s|H|\mathrm{O}\ s\rangle & \langle \mathrm{Si}\ s|H|\mathrm{Si}\ s\rangle \end{pmatrix}$$

$$2A_1: \begin{pmatrix} \langle \mathrm{O}\ p|H|\mathrm{O}\ p\rangle + 6V_1^0 & \sqrt{8}\langle \mathrm{O}\ p|H|\mathrm{Si}\ s\rangle \\ \sqrt{8}\langle \mathrm{Si}\ s|H|\mathrm{O}\ p\rangle & \langle \mathrm{Si}\ s|H|\mathrm{Si}\ s\rangle \end{pmatrix}$$

$$2F_2: \begin{pmatrix} \langle \mathrm{O}\ s|H|\mathrm{O}\ s\rangle - 2V_5^0 & \sqrt{\frac{8}{3}}\langle \mathrm{O}\ s|H|\mathrm{Si}\ p\rangle \\ \sqrt{\frac{8}{3}}\langle \mathrm{Si}\ p|H|\mathrm{O}\ s\rangle & \langle \mathrm{Si}\ p|H|\mathrm{Si}\ p\rangle \end{pmatrix}$$

$$3F_2: \begin{pmatrix} \langle \mathrm{O}\ p|H|\mathrm{O}\ p\rangle - 2V_1^0 & 4V_2^0 & \sqrt{\frac{8}{3}}\langle \mathrm{O}\ p|H|\mathrm{Si}\ p\rangle_\sigma \\ 4V_2^0 & \langle \mathrm{O}\ p|H|\mathrm{O}\ p\rangle + V_3^0 + 3V_4^0 & \sqrt{\frac{16}{3}}\langle \mathrm{O}\ p|H|\mathrm{Si}\ p\rangle_\pi \\ \sqrt{\frac{8}{3}}\langle \mathrm{Si}\ p|H|\mathrm{O}\ p\rangle_\sigma & \sqrt{\frac{16}{3}}\langle \mathrm{Si}\ p|H|\mathrm{O}\ p\rangle_\pi & \langle \mathrm{Si}\ p|H|\mathrm{Si}\ p\rangle \end{pmatrix}$$

$$1F_1: \left(\langle \mathrm{O}\ p|H|\mathrm{O}\ p\rangle - 3V_3^0 - V_4^0\right)$$

$$1E: \left(\langle \mathrm{O}\ p|H|\mathrm{O}\ p\rangle + 3V_3^0 - 3V_4^0\right)$$

we have set them both to roughly 17 eV. As the pseudopotential results show that the peak at 15 eV is not weak antibonding in character, we have made it strong antibonding. This is not completely correct either, however, and thus the character of our conduction bands is probably incorrect above 14 eV. With the eigenvalues established in this manner, we have 11 constraints on the Hamiltonian and 14 parameters. To constrain the parameterization completely, we set the orbital self-energies to their atomic values, but allow the silicon levels to shift together relative to the oxygen levels. We find that in order to fit the density of states, particularly to open up the gap, the silicon levels must be shifted *upward* between 4.5 and 7 eV, depending on what one takes for the atomic levels.

VI. BONDING NATURE OF THE GAP

One of the most distinguishing characteristics of SiO_2 is its dual ionic and covalent character. The charge on an oxygen atom is usually estimated to be -1, which easily classifies SiO_2 as an ionic material in the sense of charge transfer. On the other hand, this and other calculations show that SiO_2 possesses directional bonds and has electronic properties when disordered expected of a covalent material. In the sense of tight binding, the covalency or ionicity of a material is also reflected in the origin of its gap. In a classic ionic material, such as NaCl, the electronic levels of the neutral anion and cation are very different, so that as the atoms are brought together to form the solid, relatively little bonding occurs, and the size of the gap reflects primarily the disparity in the atomic levels. In a classical covalent material, such as silicon, the anion and cation levels are so similar (equal) that the size of the gap reflects primarily the strength of the bonding interaction. In constructing a theory of SiO_2 capable of predicting the results of large distortions, it is clearly necessary to know which picture is more correct. If one breaks a bond in a covalent material, for example, the gap region will be severely perturbed, and the result will be a dangling-bond state. In an ionic material, on the other hand, the perturbation is small and there will be no state in the gap.

The charge densities produced by the pseudopotential calculation show that the lowest conduction states of α quartz have considerable oxygen-s character. This has been interpreted previously[3,11] as oxygen 3s, the implicit understanding being that there is an accidental degeneracy of these states with the excited oxygen-3s resonance, which thus mixes in without significantly altering the energies. There are two strong arguments in favor of this picture: (a) Assuming that the O 2p level lies at the center of the lone-pair-like band, the O 3s states lies at roughly this energy. (b) The O 2s states and lower conduction bands are separated by 30 eV, an excessively large range over which to find significant oxygen-2s character. Despite these arguments, however, we believe that at least some oxygen-2s character is present in the lower conduction bands, and that its presence is important for the formation of the gap in SiO_2. The reasons are the following: (a) The atomic silicon-3s and oxygen-2p levels are approximately equal. Unless bonding of silicon s states with oxygen 2s is introduced, the gap can be opened only by *raising* the silicon levels between 4.5 and 7 eV. This is very unphysical, in light of the enormous charge transfer in SiO_2. We have, in fact, been able to take matrix elements of atomic wave functions across the pseudopotential[24] and find that the silicon-3s level lies slightly *below* the oxygen 2p. (b) The pseudowave function of the lowest conduction state is antibonding.[24] The negative phase between silicon and oxygen amplitudes appears to be necessary in order to have orthogonality to the oxygen-s bands. (c) A "reasonable" tight-binding Herman-Skillman[25] wave functions, fitting them to 2 G outside the core (distances in a.u.)

$$\psi_s \propto \exp(-0.180r^2) \ , \tag{29}$$

$$\psi_0 \propto \exp(-0.514r^2) \ . \tag{30}$$

With the Si-O-Si angle set to 180°, one obtains the two-level problem for the energies and wave functions of the lowest conduction and lowest oxygen s state indicated in the first matrix in Table II. In Table III, we list an alternate set of parameters in which the Si-3s and O-2p levels are reordered, but which gives the same energies as the parameters in Table I. This is made possible by the inclusion of a small nearest-neighbor overlap. Using the amplitudes produced by these parameters, we make bonding and antibonding combinations of the wave functions (29) and (30), square to produce charge densities, and compare these with the pseudopotential results[3] in Fig. 9. The spacing between contours is uniform within a frame, but cannot be compared between frames. Figure 9 shows that the charge densities of both the oxygen-s and lower conduction bands are consistent with the idea that the gap in SiO_2 is com-

TABLE III. Partial listing of a Hamiltonian including nearest-neighbor overlaps which produces the same density of states as the one listed in Table I.

$\langle O\ p\|H\|O\ p\rangle = -1.3$	$\langle Si\ s\|H\|Si\ s\rangle = -4.28$
$\langle O\ s\|H\|O\ s\rangle = -16.88$	
$\langle Si\ s\|H\|O\ s\rangle = -5.31$	$\langle Si\ s\|O\ s\rangle = 0.14$
$V_S^0 = -0.45$	

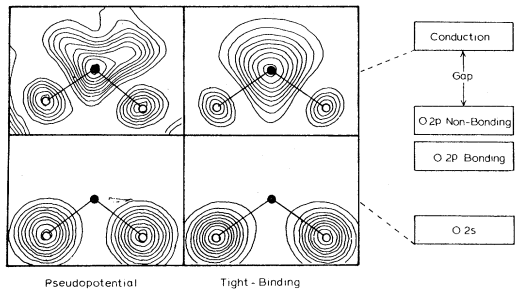

FIG. 9. Comparison between pseudopotential charge densities and those calculated using the Hamiltonian listed in Table III and the model wave functions (29) and (30).

pletely covalent. Despite the fact that the oxygen s states contain 12% silicon character, they look free of silicon because the silicon orbitals are so much more diffuse than the oxygen orbitals. The antibonding state is also in excellent agreement with pseudopotential. It contains less oxygen character than it should, however, which seems to indicate that oxygen $3s$ is participating in the state as well.

We have been able to construct an entire Hamiltonian based on atomic levels which produces densities of states virtually identical to those in Fig. 5. We have not listed its parameters, however, because including the nonorthogonality causes the Hamiltonian to be severely overparameterized. It is likely, however, that such nonorthogonal Hamiltonians are closer to the truth as regards the silicon dangling bond states than is the one listed in Table I.

VII. DISORDER

The major differences between the densities of states of crystalline and amorphous *silicon* have been attributed[26] to differences in topology. As was discussed in Sec. II, the topological randomness of the disordered system tends to be modeled well by the topological neutrality of the Bethe lattice, so that one can assess the effects of disorder by comparing the crystal and Bethe-lattice densities of states. Amorphous silicon is described approximately by the Hamiltonian[18] in Sec. III. Thus, the differences seen in Fig. 5 between the crystal and Bethe-lattice strong-bonding bands are analogous to the differences between crystalline and amorphous silicon. The three-peak structure seen in this band in α quartz has been shown by Thorpe[27] to be due to the presence of six- and eightfold rings of bonds. In silicon, only sixfold rings, are present, thus reducing the number of peaks to two.[26] Nevertheless, the disappearance of this structure when the material is made amorphous, which is evident in Fig. 4, is the same phenomenon in both materials, and provides additional evidence that the bonding picture of SiO_2 is the correct one. While this structure has not yet been resolved in either the oxygen-s or lower conduction bands, it is present in the crystal and should also be found to disappear when the solid is made amorphous.

While bond lengths remain fairly constant in the amorphous material, bond-angle fluctuations, particularly of the Si-O-Si angle, are known[28] to be prevalent. An obvious question to ask is whether these fluctuations are the cause of the disparity in the lone-pair-like bands between the upper and lower halves of Fig. 4. To the extent a nearest-neighbor description is accurate, this is *not* the case. The effect of opening and closing the Si-O-Si angle, for example, may be assessed by comparing the lone-pair-like region in Fig. 5 with the top of Fig. 8. Changing this angle appears to rob states from one edge of this band and transport them to the other, without changing the bandwidth or putting states in the center. This is caused by a change in the splitting between the weak-bonding and lone-pair bond orbitals. In addition, distorting the SiO_4 tetrahedron tends to increase the mean-square splitting of the lone-pair orbitals, and thus the width of the band. As the tight-binding density of states looks more like the amorphous XPS[20] than that of the crystal, a likely explanation is that these effects are caused by distant-neighbor interactions which are disrupted in the glass.

The region of the density of states which should be severely affected by bond-angle disorder is the conduction-band edge. When the Si-O-Si angle is 180°, the weak-antibonding bond orbital, which forms the bottom of the conduction band, contains no oxygen-p character. As this angle is bent, progressively more oxygen p is incorporated into the state, resulting in *upward* motion of this state by 2 eV upon reaching the nominal α-quartz angle of 144°. The magnitude of this effect is determined by the strength of the bonding interaction, which can be determined fairly unambiguously from the splitting between the strong-bonding and lone-pair-like bands. Pantelides and Harrison[3] have shown that the interaction of this state with the oxygen p states should scale as $\cos\frac{1}{2}\theta)$. Thus the fluctuations of about $\pm 10°$ seen in this angle in amorphous SiO_2 (Ref. 28) should result in roughly 0.5-eV band tailing at the conduction-band edge. We cannot describe the mobility edge of this system at present. It would be pointed out, however, that this is inherently a simple problem with diagonal disorder and constant nearest-neighbor transfer integrals which might be investigated numerically.

VIII. SUMMARY

In this paper, we have developed a picture of the electronic states of SiO_2 in which periodicity plays no

role. Using the Bethe lattice as a structural model for the material, we have been able to attribute quantitatively a number of its properties to the integrity of the local atomic environment, particularly the SiO_4 tetrahedron, in its structure. The most significant of these are the overall shapes of the bands and the dipole selection rule forbidding the first optical transitions. We have also shown that SiO_2 may have a covalent gap, the great size of which is directly attributable to the presence of oxygen-2*s* character in the lower conduction bands. As regards disorder, we have made two major points: (a) the major differences between the densities of states of crystalline and amorphous SiO_2 have analogs in silicon, and (b) there should be considerable band tailing from the conduction bands in the glass.

ACKNOWLEDGMENTS

This research was supported in part by the U.S. Navy, ONR Grant No. N0014-77-C-0132. Two of us (R. B. L. and J. D. J.) should like to acknowlege receipts of IBM and Alfred P. Sloan Fellowships, respectively. We are particularly grateful to M. Schlüter for making his self-consistent potential and wave functions available to us. We should also like to thank R. Pollak for providing us with his photoemission spectra.

---

*Current address: Bell Telephone Laboratories, Murray Hill, N.J. 07974.

[1]For extensive references to theoretical and experimental work, see the review articles by A. R. Ruffa, J. Non-Crystal. Solids 13, 37 (1973); D. L. Griscom, J. Non-Crystal. Solids 24, 155 (1977).

[2]S. T. Pantelides and W. A. Harrison, Phys. Rev. B 13, 2667 (1976).

[3]J. R. Chelikowsky and M. Schlüter, Phys. Rev. B 15, 4020 (1977); M. Schlüter and J. R. Chelikowsky, Solid State Commun. 21, 381 (1977).

[4]K. L. Yip and W. B. Fowler, Phys. Rev. B 10, 1400 (1974).

[5]P. M. Schneider and W. B. Fowler, Phys. Rev. Lett. 36, 425 (1976).

[6]E. Calabrese and W. B. Fowler, Phys. Rev. B 18, 2888 (1978).

[7]S. Ciraci and I. P. Batra, Phys. Rev. B 15, 4923 (1977).

[8]J. A. Bennett and L. M. Roth, Phys. Rev. B 4, 2686 (1971); J. Phys. Chem. Solids 32, 1251 (1971).

[9]J. A. Tossell, D. J. Vaughan, and K. H. Johnson, Chem. Phys. Lett. 20, 329 (1973).

[10]T. L. Gilbert, W. J. Stevens, H. Schrenk, M. Yoshimine, and P. S. Bagus, Phys. Rev. B 8, 5977 (1973).

[11]N. F. Mott, Adv. Phys. 26, 363, (1977).

[12]Many useful references may be found in *The Physics of SiO_2 and its Interfaces,* edited by S. T. Pantelides (Pergamon, New York, 1978).

[13]J. D. Joannopoulos and F. Yndurain, Phys. Rev. B 10, 5164 (1974).

[14]C. Domb, Adv. Phys. 9, 145 (1960).

[15]R. B. Laughlin and J. D. Joannopoulos, Phys. Rev. B 16, 2942 (1977).

[16]R. B. Laughlin and J. D. Joannopoulos, Phys. Rev. B 17, 2790 (1978).

[17]J. D. Joannopoulos, J. Non-Crystal Solids 32, 241 (1979).

[18]M. F. Thorpe and D. Weaire, Phys. Rev. B 4, 3518 (1971).

[19]F. Yndurain, Solid State Commun. 27, 75 (1978).

[20]B. Fischer, R. A. Pollak, T. H. DiStefano, and W. D. Grobman, Phys. Rev. B 15, 3193 (1977).

[21]H. R. Phillip, Solid State Commun. 4, 73 (1966); J. Phys. Chem. Solid 32, 1935 (1971).

[22]E. Loh, Solid State Commun. 2, 269 (1964).

[23]G. Klein and H. U. Chun, Phys. Status Solidi B 49, 167 (1972).

[24]M. Schlüter (private communication).

[25]F. Herman and S. Skillman, *Atomic Structure Tables* (Prentice-Hall, Englewood Cliffs, 1963).

[26]J. D. Joannopoulos and M. L. Cohen, in *Solid State Physics* edited by H. Ehrenreich (Academic, New York,1976), Vol. 31.

[27]M. Thorpe, Ref. 14, p. 116.

[28]R. L. Mozzi and B. E. Warren, J. Appl. Crystal. 2, 164 (1969).